Enzyme and Microbial Technology 142 (2020) 109676

Contents lists available at ScienceDirect

Enzyme and Microbial Technology

journal homepage: www.elsevier.com/locate/enzmictec

The effects on antioxidant enzymes of PMMA/hydroxyapatite nanocomposites/composites

Serap Doğan [a,*], Taner Özcan [b], Mehmet Doğan [c], Yasemin Turhan [c]

[a] Balıkesir University, Faculty of Science and Literature, Department of Molecular Biology and Genetic, Balıkesir, Turkey
[b] Balıkesir University, Faculty of Necatibey Education, Department of Biology Education, Balıkesir, Turkey
[c] Balıkesir University, Faculty of Science and Literature, Department of Chemistry, Balıkesir, Turkey

ARTICLE INFO

Keywords:
PMMA
nHA
Nanocomposites
Composites
Antioxidant enzymes
Biocompatibility

ABSTRACT

In this study, polymer-ceramic nanocomposites and/or composites were prepared by solution removal method using poly(methylmethacrylat) (PMMA) and nano-hydroxyapatite (nHA). They were characterized using X-ray diffraction (XRD), Fourier transform infrared-attenuated total reflection spectroscopy (FTIR-ATR), and differential thermal analysis/thermogravimetry (DTA/TG). Their effects and biocompatibilities on antioxidant enzymes were also investigated in detail. It has been shown that nHA was dramatically dispersed at nanoscale in the polymer matrix. The interaction occurred between —OH groups of nHA and carbonyl groups of polymer and introduction of ceramic into the polymer matrix generally resulted in an increase in thermal stability. Nanocomposites and composites had different effects on enzyme activities. Samples synthesized in acetone increased enzyme activities for glutathione reductase (GR) and glucose-6 phosphate dehydrogenase (G6PD) enzymes, while inhibiting glutathione peroxidase (GPx) and catalase (CAT) enzyme activities. On the other hand, samples synthesized in tetrahydrofuran (THF) exhibited inhibitory behavior for G6PD and CAT enzymes. The samples synthesized in different media did not show any regularity on enzyme activities. The nanocomposites and/or composites prepared in acetone media were better hemocompatible than those in THF.

1. Introduction

As can be clearly seen, studies are accelerating constantly on the development of new technological biomaterials that can adapt when interacting with the biological systems for the treatment of hard and soft tissue damages caused by accidents. Biomaterials commonly used for this purpose are divided into four main groups: metals, ceramics, polymers and composites. Each material has its own application area. However, these materials have some disadvantages due to their intrinsic structural features such as being fragile and corrosive, difficulties in processing, slow degradation rates, and reaction products being toxic. Ceramic based biomaterials are the most widely preferred materials because they are biologically active. Bone is a natural composite material in which the collagen fibers pass through hydroxyapatite. Inorganic calcium phosphate based hydroxyapatite, which makes up 70 % of bone tissue by weight, is a bioceramic material used in medicine and dentistry. It is also used for making various prostheses as artificial bone, repairing cracked and broken bones, and coating metallic biomaterials due to its biocompatibility. However, due to its hardness, fragility and poor mechanical properties, its use alone in implant materials is quite limited. Some weak properties of hydroxyapatite can be improved with the help of nanocomposites prepared using biocompatible polymers [1–3].

In the literature, there are studies on the synthesis of nanocomposites of hydroxyapatite with different polymers. Zhang et al. (2020) prepared polyuria/hydroxyapatite nanocomposites by in-situ polymerization of polycarbodimide modified diphenylmethane diisocyanate, and investigated mechanical, thermal, and biocompatibility properties of nanocomposites [4]. Zhou et al. (2019) were firstly synthesized PVA-GMA and subsequently photocrosslinked PVA-GMA/Hap nanocomposite hydrogels. They investigated the effects of the Hap on the gel-formation, gel microstructures, and mechanical properties of the nano-composite hydrogels and also *in vitro* evaluated the cell adhesion of nanocomposite hydrogels as articular cartilage replacements by using mouse fibroblasts (L929) as a model cell line [5]. Banerjee et al. (2018) prepared antimicrobial and biocompatible fluorescent hydroxyapatite-chitosan nanocomposite films for biomedical application and characterized by UV/Visible spectroscopy, X-ray diffraction,

* Corresponding author.
E-mail address: sdogan@balikesir.edu.tr (S. Doğan).

https://doi.org/10.1016/j.enzmictec.2020.109676
Received 28 June 2020; Received in revised form 20 September 2020; Accepted 21 September 2020
Available online 28 September 2020

Fourier transform infrared spectroscopy, photoluminiscence spectroscopy and Field emission scanning electron microscopy [6]. Shirali et al. (2017) used to a combination of elastic poly(butylene succinate-co-ethylene terephthalate) and rigid nano-hydroxyapatite to prepare an in-situ synthesized nanocomposite mimicing bone structure. They investigated the microstructure, morphology, and dispersion of nanoparticles in the nanocomposites using proton nuclear magnetic resonance, scanning electron microscopy, and transmission electron microscopy [7].

Poly(methylmethacrylate) PMMA, one of the polymers used as a matrix in nanocomposites and/or composites, is known as a biocompatible polymer. In the literature, there are also different studies on PMMA/hydroxyapatite nanocomposite and/or composites. Wijesinghe et al. (2019) synthesized a hydroxyapatite/poly(methylmethacrylate) nanocomposite by a novel, simple and industrially applicable method using dolomite and found that HA in the synthesized PMMA nanocomposite was 30 nm in size and had a spherical morphology with 84 % yield [8]. Tihan et al. (2009) studied effect of hydrophilic-hydrophobic balance on biocompatibility of (PMMA)-HA composites [9]. Zhang et al. (2008) characterized hydroxyapatite/PMMA nanocomposites for provisional dental implant restoration and studied human gingival fibroblasts biocompatibility [10]. In our previous studies, we investigated hemocompatibility, cytotoxicity, and genotoxicity of poly(methylmethacrylate)/nanohydroxyapatite nanocomposites synthesized by melt blending method [2] and some biological properties of PMMA/modified-nanohydroxyapatite nanocomposites [1].

According to the best of our knowledge, there is no study in the literature on the interaction of these materials with antioxidant stress enzymes. Therefore, the main purposes of this study were to synthesize PMMA/nHA nanocomposites and/or composites according to the solvent removal method and first time to investigate how they affect as inhibitor or activator the antioxidant enzyme activities such as glutathione peroxidase (GPx), glutathione reductase (GR), glutathione-s-transferase (GST), glucose-6 phosphate dehydrogenase (G6PD), catalase (CAT) and superoxide dismutase (SOD) in the human body by in vitro experiments. Synthesized samples were characterized using X-ray diffraction (XRD), Fourier transform infrared-attenuated total reflection spectroscopy (FTIR-ATR), and differential thermal analysis/thermogravimetry (DTA/TG). Finally, the interactions of the bionanocomposites with the antioxidant enzymes were investigated in detail. With this study, the inhibitory and/or activator effects of nanocomposites and/or composites on each antioxidant enzyme were revealed and discussed. Also, the reactions between the action mechanisms of these enzymes were investigated.

2. Material and method

2.1. Material

The chemicals used in the study were purchased from Merck and Sigma. They were analytical grade and used without further purification. Enzyme activities were measured using PerkinElmer Lambda 25 UV–vis spectrophotometer.

2.2. Methods

2.2.1. Hemolysate preparation

Venous blood was taken with sterile citrated tubes from healthy young individuals in the age range of 17–22 for erythrocyte antioxidant enzyme activity measurements. After the bloods were transferred to eppendorf tubes, it was first centrifuged at +4 °C for 15 min at 2500 rpm. The plasma remaining in the upper part was carefully discarded. The remaining part was washed out three times at 2500 rpm for 5 min at +4 °C with 0.16 M KCl, diluted 1/5 with cold pure water, centrifuged at 10,000 rpm for 30 min at +4 °C and erythrocytes were disintegrated [11].

The sample obtained was divided into two parts. The first part was used for control purposes in enzyme activities. About 5 × 5 mm in size (about 0.0022 *g*) cut nanocomposite and/or composite samples were added to the second part and waited for 1 h. Then, this mixture was centrifuged at 10,000 rpm for 30 min. The enzyme activities were measured and compared to the control group. All experiments were performed in three times. Standard deviations were calculated and given in tables and figures.

2.2.2. Nanocomposite synthesis

Solvent selection is an important parameter in the preparation of nanocomposites. In this study, a suitable solvent was chosen for each system (polymer + ceramic + solvent) in which the filler was completely dispersed and the polymer was completely dissolved. The ceramic and polymer were placed in reaction vessels separately in the appropriate solvent and mixed for 2 h at room temperature on a magnetic stirrer. The ceramic-solvent suspension was kept in the ultrasonic bath for 20 min. The polymer solution and ceramic suspension were combined and mixed on a magnetic stirrer for 24 h. Samples were taken into Petri dishes and their solvents were removed in an oven at 50 °C [12].

2.3. Characterization of nanocomposites

2.3.1. X-ray diffraction (XRD)

XRD pattern of the samples were taken using an Analytical Philips X'Pert-Pro X-ray diffractometer equipped with a back monochromator operating at 40 kV and a copper cathode as the X-ray source (λ =1.54 Å).

2.3.2. FTIR-ATR analysis

FTIR-ATR spectra of the samples were taken using PerkinElmer Spectrum 100 model Fourier transform infrared spectroscopy in the wavenumber range of 600–4000 cm^{-1}.

2.3.3. Thermogravimetric analysis (DTA/TG)

Thermal properties of PMMA/HA nanocomposites were examined under N_2 atmosphere using PerkinElmer Diamod DTA/TG thermal analyzer in the temperature range of 25−600 °C.

2.4. Determination of antioxidant enzyme activities

2.4.1. Measurement of G6PD enzyme activity

G6PD enzyme activity was spectrophotometrically measured as a result of the absorption increase of NADPH formed at the end of the reaction at 340 nm wavelength. Except for G6P, all chemicals given in Table 1 were incubated at 37 °C for 10 min. Then, 300 μL of G6P was added to the sample and reference cuvette and the absorbance was recorded at 340 nm for 2 min. One enzyme unit was defined as the enzyme amount reducing 1 μmol $NADP^+$ per minute [13].

2.4.2. Measurement of GPx enzyme activity

Oxidation of GSH to GSSG occurs in the presence of t-butylhydroperoxide with GPx. The method is based on the principle that the difference in the absorbance value at 340 nm of NADPH oxidized to NADP in response to the reduction of GSH by GR enzyme to GSH is measured against time. GPx activity was measured using the contents given in Table 1. After adding of all chemicals into sample and reference cuvette, they were allowed to incubate at 37 °C for 10 min. Then, t-butylhydroperoxide was added into the sample cuvette and the activity against the reference was measured. One unit of GPx represented 1 μg GSH utilized per minute [14].

2.4.3. Measurement of GR enzyme activity

GR catalyzes the reduction of GSSG to GSH by NADPH. The enzyme activity was determined by measuring the absorbance difference of the NAD(P)H oxidized during the reaction at a wavelength of 340 nm at 37 °C. GR activity was measured using the contents given in Table 1. One

Table 1
The substances used for the antioxidant enzyme activity measurements.

Antioxidant enzymes	Chemicals
G6PD	Distilled water Tris–EDTA $MgCl_2$ $NADP^+$ Hemolysate G6P Tris-EDTA GSH
GPx	Glutathione reductase NADPH Hemolysate Distilled water t-butylhydroperoxide
GR	Distilled water Tris–EDTA NADPH GSSG Hemolysate
GST	Phosphate buffer CDNB GSH Hemolysate
CAT	Phosphate buffer H_2O_2 Hemolysate
SOD	Phosphate buffer Xanthine oxidase Xanthine INT Hemolysate

unit of GR was defined as the quantity of NADPH consumed per minute, which catalyzed the reduction of 1 mM of GSSG [13].

2.4.4. Measurement of GST enzyme activity

GST catalyzes the reaction between 1-chloro-2,4-dinitrobenzene (CDNB) and the glutathione-SH group. Enzyme activity was determined by measuring the amount of enzyme catalyzing 1 μmol of S-2,4-dinitrophenylglutathione formed per min at 340 nm and 37 °C using GSH and CDNB. GST activity was measured using the contents given in Table 1 [14].

2.4.5. Measurement of CAT enzyme activity

CAT catalyzes the destruction of water and molecular oxygen by H_2O_2. The degradation rate of the enzyme at 240 nm was spectrophotometrically measured by utilizing the light absorptivity of H_2O_2. CAT activity was measured using the content given in Table 1. After adding of the chemicals into the reference and sample cuvette, activity against the reference was measured for 5 min at 240 nm and the decrease in absorbance was recorded at 1 min intervals. One unit of CAT represented the amount of enzyme that decomposes 1 μmol of H_2O_2 per minute [15].

2.4.6. Measurement of SOD enzyme activity

SOD enzyme accelerates the dismutation of toxic superoxide radicals to hydrogen peroxide and molecular oxygen (O_2), which are formed during the production of oxidative energy. In the method, superoxide radicals which react with 2-[4-iodophenyl]-3-[4-nitrophenol]-5-phenyltetrazolium chloride (INT) and form a red colored spray pigment, are produced using xanthine and xanthine oxidase (XOD). The enzyme activity measurement was based on the inhibition of the reaction by SOD enzyme at 505 nm in the medium. SOD activity was measured using the contents given in Table 1 [16,17].

2.5. Hemocompatibility test

The hemocompatibility test of polymer and biomaterial was spectrophotometrically determined. Human blood (2 mL) was taken into tubes with citrate to avoid coagulation. Anticoagulated blood was diluted 1/5 with saline solution. 0.2 mL of diluted blood for positive control was added to 0.5 mL of 0.01 M HCl, diluted to 10 mL and incubated for 1 h at 37 °C. Similarly, 0.2 mL of diluted blood for negative control was diluted to 10 mL with the addition of normal salt solution and incubated at 37 °C for 1 h. The mixture consisting of 0.2 mL of diluted blood in the centrifuge tube and 9.8 mL of saline solution was incubated at 37 °C for 30 min to reach equilibrium temperature. Samples with 5 × 5 mm (0.0022 *g*) in size were taken into centrifuge tubes containing the blood-salt mixture and incubated at 37 °C for 1 h. After incubation, all sample solutions were centrifuged at 6000 rpm for 10 min and after the supernatant fluid was carefully removed, it was placed in the cuvette for spectrophotometric analysis. Optical densities of the incubated sample solutions were measured using a UV–vis spectrophotometer at 545 nm.

$$\text{Hemolysis } \% = \frac{\left[OD_{test} - OD_{negative}\right]}{\left[OD_{positive} - OD_{negative}\right]} \times 100 \quad (1)$$

Where OD_{test} is the optical density of the sample solution, $OD_{positive}$ is the optical density of the positive control and $OD_{negative}$ is the optical density of the negative control. If hemolysis percent is 5% and below, nanocomposite is considered to be hemocompatible. If hemolysis percent is 10 % and below, it is considered to be biocompatible [18].

3. Results and discussion

The characterization results of the synthesized biomaterials, interactions of these materials with GPx, GR, GST, G6PD, CAT, and SOD antioxidant enzymes, and the results of biocompatibility tests determined from the percentage of hemolysis in the blood have been discussed as follows;

3.1. Characterization

Characterization of biomaterials was carried out by means of patterns, spectra and thermograms obtained from XRD, FTIR-ATR and DTA/TG devices, respectively.

3.1.1. XRD analysis

From the XRD patterns of PMMA/HA (2.5 wt%) nanocomposites prepared in different solvent systems, the characteristic peaks of PMMA were observed at $2\theta = 14.83$ and 26.71° and those of hydroxyapatite at $2\theta = 31.42$, 32.58 and 33.82° (figure not shown). The dispersion of hydroxyapatite in the polymer matrix was evaluated by means of these peaks. This pattern also shows that PMMA has a semi-crystalline structure [19]. XRD patterns of nanocomposites show that hydroxyapatite is distributed in the PMMA matrix and the solvent type does not form a significant difference in XRD patterns. For this reason, the choice of solvent in nanocomposite synthesis was determined by evaluating thermal stability, since there was no difference in XRD patterns after considering the solubility parameters. In addition, the semi-crystalline structure of PMMA with the addition of hydroxyapatite into the polymer matrix has turned into an amorphous structure [20]. Fig. 1 shows the XRD patterns of PMMA/HA nanocomposites and composites prepared in different amounts of hydroxyapatite in THF medium. As seen from these patterns, characteristic peaks of HA in nanocomposites begin to emerge with increasing amount of hydroxyapatite. This result showed that some amount of HA was distributed in the PMMA matrix and some were agglomerated without dispersion. XRD patterns of PMMA/HA composites prepared in different hydroxyapatite amounts in THF medium show characteristic peaks of hydroxyapatite. In addition, it is seen

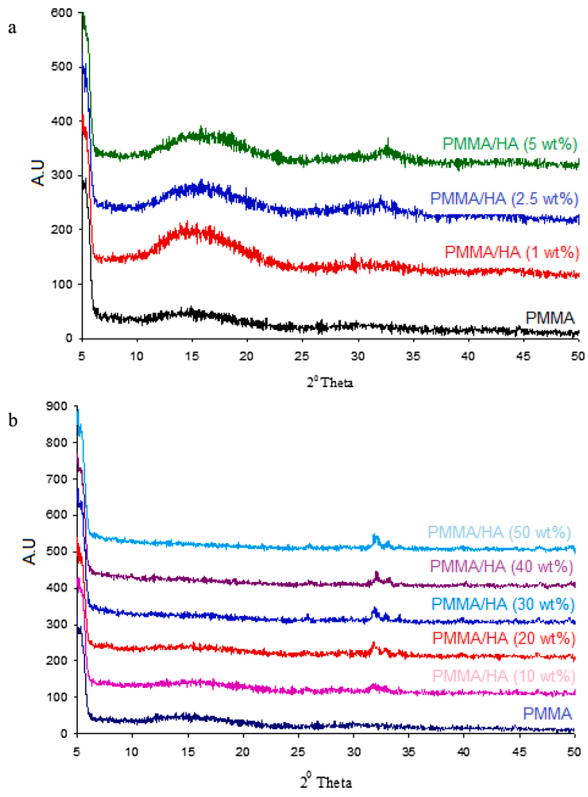

Fig. 1. XRD patterns of PMMA/HA a) nanocomposites and b) composites prepared in THF solvent.

that the percentage of crystallinity decreases as the amount of hydroxyapatite in composite increases. From the XRD patterns of PMMA/HA nanocomposites prepared in different amounts of hydroxyapatite in acetone medium (figure not shown), it has been realized that HA was well dispersed in the PMMA matrix in nanocomposites of 1 and 2.5 wt%, while some of the HA remained agglomerated in nanocomposite of 5 wt%. Due to the high amount of added HA in composites, characteristic peaks of HA were observed in XRD patterns. This indicates that HA was not well dispersed in the polymer matrix and agglomerates were formed.

3.1.2. FTIR-ATR analysis

In FTIR-ATR spectrum of hydroxyapatite (figure not shown), the peak observed at 3573 cm^{-1} belongs to the hydroxyl (—OH) group, the peaks at 1455 and 1413 cm^{-1} belong to CO_3 group, and the peaks at 1048, 961 and 874 cm^{-1} belong to the PO_4^{3} group [21]. In FTIR-ATR spectrum of PMMA, the peak at 2950 cm^{-1} belongs to the aliphatic —CH_2 group, the peak at 1722 cm^{-1} belongs to the carbonyl group (C═O), and peaks at 1239 and 987 cm^{-1} belongs to ester bonds [22].

FTIR-ATR spectra of nanocomposites give important information about interactions between PMMA polymer matrix and filler. The indication of these interactions manifested itself as new peaks and shifts of PMMA polymer peaks to lower or higher wavenumbers FTIR-ATR spectra. Fig. 2a and b indicates FTIR-ATR spectra of PMMA/HA nanocomposites and composites synthesized in different amounts of hydroxyapatite in THF and acetone (Figure not shown) medium. The hydroxyl peak at 3573 cm^{-1} of hydroxyapatite was not observed in these spectra due to interaction of hydroxyl groups in hydroxyapatite with organic polymers [21]. The peaks at 2995, 2950, 1722 and 1434 cm^{-1} of PMMA in the nanocomposite were shifted to higher or lower wavenumbers. From these results it can be argued that the polymer matrix interacts with hydroxyapatite and generally occurs between the —OH groups of HA and the carbonyl groups of PMMA. In the FTIR-ATR spectra of composites, the characteristic peaks of PMMA did not change much as in nanocomposites.

3.1.3. DTA/TG analysis

PMMA degrades in 2 steps (Figure not shown). The temperatures at which the maximum mass losses occur are 292 and 385.5 °C. It is stated in the literature that there are three radical formation processes for the degradation of PMMA. The first (100–200 °C) is ascribed to the weak head–head linkages in the main chain. The second (200–300 °C) is terminal vinyl group decomposition, and the third (300–400 °C) is due to the random scission of polymer main chain [23]. Depolymerization, which occurs with its radical formation, is the main degradation process of PMMA. Side group eliminations and polyenes occur [24,25]. From the thermograms, no mass loss occurred in the temperature range of 155−220 °C, hence no radical formation occurred in the first process. In the second and third processes, PMMA has degraded. Unlike PMMA, in these curves, a new mass loss occurs in the temperature range of 100−200 °C due to the trapping of the solvent in the nanocomposites. From the results given in Table 2, nanocomposites synthesized in THF and acetone media have the highest thermal stability. Also, since the evaporation temperature of acetone is low, it is less present in the solvent matrix. Fig. 3a and b show TG and d[TG] thermograms of PMMA/HA nanocomposites/composites synthesized in different HA amounts in THF medium. As can be seen from these thermograms, although these was no improvement realized in T_x temperatures, T_{max} temperatures were observed to increase especially for PMMA/HA (2.5 wt%) nanocomposite. In addition, the residual amount has also increased. When Table 2 is examined for composites, it was found that additional mass losses occurred at various temperatures. In general, T_x temperatures and residual amounts increase (23 and 12 °C increase in T_{max1} and T_{max2} temperature, respectively). Zhao and Zhang (2008) synthesized polyurethane/hydroxyapatite nanocomposites using polymerization method. From thermogravimetric analysis, nanocomposites have been shown to have higher thermal stability than pure polyurethane. They attributed this increase in thermal stability to crosslink formation in polyurethane and to hydrogen bonds formed between amide groups (—NH—CO—O—) in polyurethane and hydroxyl groups in hydroxyapatite [26]. According to the results obtained from FTIR-ATR analysis, the increase in thermal stability can be attributed to hydrogen bonds formed between the —OH groups in hydroxyapatite and carbonyl groups in PMMA. When TG and d[TG] thermograms of PMMA/HA nanocomposites/composites synthesized in different amounts of HA in acetone medium were examined (Figure not shown), the addition of hydroxyapatite into PMMA matrix in acetone medium did not cause a significant increase in thermal stability. It just changed the T_{max1} temperature of the first degradation. Over 400 °C, composites are thermally more stable than pure polymer. It has been observed that the addition of hydroxyapatite into the PMMA matrix changes the degradation mechanism of PMMA. Additional mass losses occurred due to solvent at low temperatures. Also, because composites contain more hydroxyapatite than nanocomposite, the residual amounts were found to be quite high. In fact, the residual amount which is in the range of 20–30 % and T_{80} temperature was not observed for some samples. When comparing nanocomposites synthesized in THF and acetone media, it can be said that hydroxyapatite is better dispersed in the PMMA matrix in the THF medium, and the nanocomposites prepared in the THF medium are more thermally stable.

3.2. Effect of biomaterials on enzyme activity

Fig. 4 shows the effect of biomaterials on antioxidant enzyme activities. There was no regular increase or decrease in glutathione peroxidase enzyme activity by increasing of the HA amount for biomaterials synthesized in THF medium. Compared to the control sample, enzyme activity decreased for nanocomposites or composites containing 1, 10, 20 and 30 wt% HA, and conversely, it increased for nanocomposites or composites containing 2.5, 5, 40, and 50 wt% HA. The

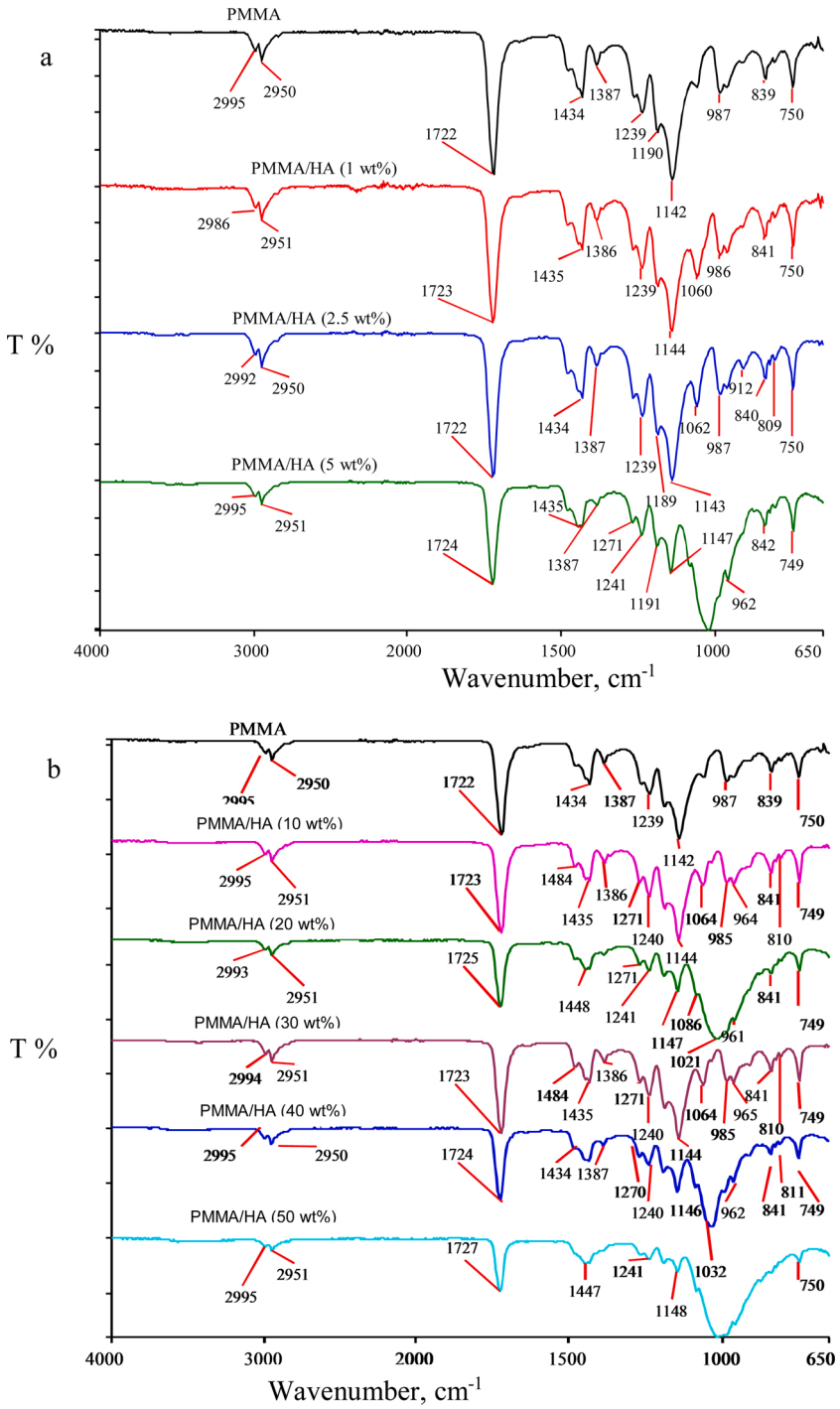

Fig. 2. FTIR spectra of PMMA/HA a) nanocomposites and b) composites prepared in THF solvent.

biggest decrease is 30 wt% of composite (decrease 37.5 %), the highest increase is 40 wt% of composite (increase 43.75 %). This indicates that the change in the activity of the enzyme does not depend on the amount of HA in the PMMA/HA nanocomposite and/or composites. All biomaterials synthesized using acetone as a solvent reduced the activity of the glutathione peroxidase enzyme. The maximum enzyme activity decreased about 40 % for composite containing 40 wt% HA. The ratios of other samples affecting activity are close to each other. According to these results, it can be said that PMMA/HA nanocomposites and/or composites synthesized in acetone medium inhibit the activity of the glutathione peroxidase enzyme. Considering the effects of PMMA/HA nanocomposites and/or composites synthesized in THF and acetone on glutathione reductase enzyme activity, samples containing 10 and 30 % HA by weight in the THF medium increase glutathione reductase enzyme activity (4.35 % and 8.7 % respectively). On the other hand, other samples reduce enzyme activity. However, it can be argued that nanocomposites and/or composites generally have no significant effect on glutathione reductase enzyme activity. PMMA/HA nanocomposites and/or composites synthesized using acetone as a solvent increased the glutathione reductase enzyme activity. The highest increases in enzyme activity were observed for composites containing 30 and 40 wt% HA. This result indicates that PMMA/HA nanocomposites and/or composites act as an activator for the glutathione reductase enzyme. Enzyme activators are molecules that bind to enzymes and increase their activity.

Table 2
DTA/TG analysis data of PMMA and PMMA/HA nanocomposites and/or composites.

Samples	Solvent systems	T_5 (°C)	T_{10} (°C)	T_{30} (°C)	T_{50} (°C)	T_{80} (°C)	T_{max1} (°C)	T_{max2} (°C)	Residue (%) (600 °C)
PMMA	——	326.1	346.3	369.1	380.1	397.2	292.2	385.6	0
PMMA/HA (1 wt%)	THF	145.0	184.4	357.2	375.9	395.4	288.2	384.2	0.48
PMMA/HA (2.5 wt%)	THF	158.3	267.5	363.2	378.9	397.4	296.2	386.2	2.23
PMMA/HA (2.5 wt%)	Acetone	245.3	281.5	360.1	377.3	396.7	298.9	384.3	2.44
PMMA/HA (2.5 wt%)	Chloroform + acetone	171.5	264.4	364.4	379.0	398.0	286.6	385.5	2.44
PMMA/HA (2.5 wt%)	Acetone + THF	176.1	217.5	357.6	378.1	399.6	299.2	390.6	1.95
PMMA/HA (2.5 wt%)	Chloroform + THF	155.4	193.4	361.7	378.8	398.3	282.2	384.4	1.38
PMMA/HA (5 wt%)	THF	162.6	192.5	350.0	375.8	396.5	280.3	386.6	3.88
PMMA/HA (10 wt%)	THF	167.4	201.4	356.2	378.3	401.9	280.3	387.5	8.04
PMMA/HA (20 wt%)	THF	163.9	217.3	352.0	379.8	406.0	298.7	390.2	9.96
PMMA/HA (30 wt%)	THF	178.9	247.0	361.9	389.7	——	298.9	395.5	23.25
PMMA/HA (40 wt%)	THF	217.3	273.0	333.0	379.6	——	296.5	389.6	27.97
PMMA/HA (50 wt%)	THF	191.2	291.7	345.3	385.7	——	303.3	388.4	33.19
PMMA/HA (1 wt%)	Acetone	262.6	329.8	367.2	380.0	396.5	290.7	384.2	0.14
PMMA/HA (5 wt%)	Acetone	239.6	267.0	343.7	371.1	394.5	302.3	383.6	5.24
PMMA/HA (10 wt%)	Acetone	223.1	271.0	337.0	370.3	398.9	301.5	383.6	8.88
PMMA/HA (20 wt%)	Acetone	224.4	266.4	317.1	365.4	405.7	299.2	385.3	14.49
PMMA/HA (30 wt%)	Acetone	164.1	250.6	295.1	336.4	419.0	295.5	384.7	18.81
PMMA/HA (40 wt%)	Acetone	181.9	259.4	300.9	347.3	——	294.2	384.1	27.98
PMMA/HA (50 wt%)	Acetone	251.2	266.4	300.3	351.0	——	281.0	382.3	34.09

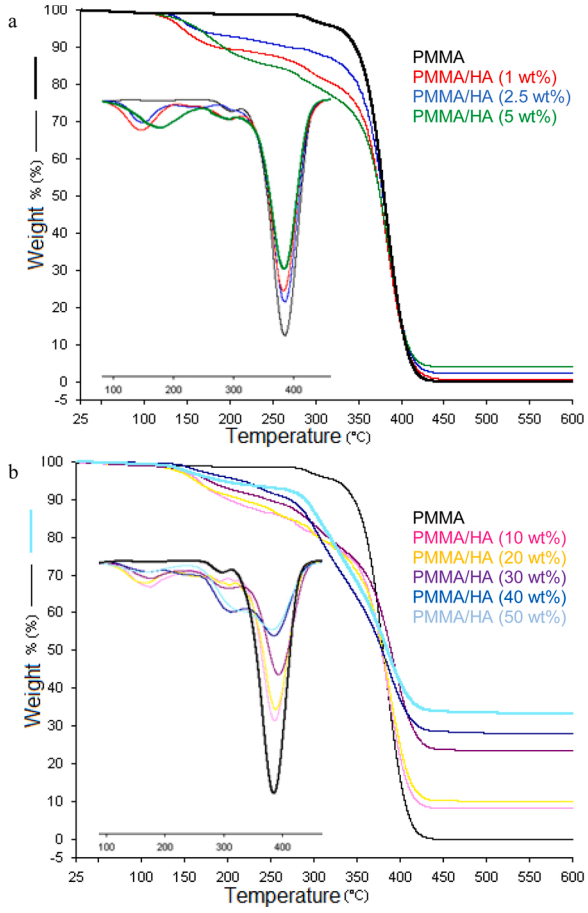

Fig. 3. TG thermograms of PMMA/HA a) nanocomposites and b) composites prepared in THF solvent.

They are the opposite of enzyme inhibitors. PMMA/HA nanocomposites and/or composites generally increase glutathione s-transferase enzyme activity. However, this increase is not very high. The effects of PMMA/HA nanocomposite and/or composites on glucose-6 phosphate dehydrogenase enzyme activity are given in Fig. 4. The changes in the enzyme activity of the synthesized nanocomposite and/or composites are similar. However, when the effect of the samples synthesized in THF medium on the enzyme activity is compared with the control group, it is seen that all samples decrease the enzyme activity and the samples synthesized in acetone medium also increase. It can be seen from Fig. 4 that nanocomposites and/or composites slightly decrease catalase enzyme activity. The highest decrease was observed in the PMMA/HA composite containing 40 wt% HA which was prepared using THF as a solvent. The lowest decrease was determined in the PMMA/HA nanocomposite containing 1 wt% HA. It is also realized that the decrease in the activity of the enzyme is not proportional to the amount of HA. From the above explanations, it can be concluded that the samples synthesized in THF medium inhibit the catalase enzyme more than the samples synthesized in acetone medium. The effects of nanocomposites and/or composites synthesized in THF and acetone on superoxide dismutase enzyme activity differ from each other. Samples that the enzyme activity reduce the most are PMMA/HA nanocomposites containing 1 and 2.5 wt % HA synthesized using acetone as the solvent. The highest reduction in those synthesized in THF medium was achieved for PMMA/HA nanocomposite containing 2.5 wt% HA. On the other hand, it can be seen that some of the synthesized samples also act as activators on the superoxide dismutase enzyme. For example, composites containing 20, 30 and 40 wt% HA synthesized in THF medium increased the enzyme activity. Samples containing 5 and 20 wt% HA synthesized in acetone medium also positively affected SOD activity. These results show that the amount of HA in nanocomposites and/or composites is not very important in influencing superoxide dismutase enzyme activity.

3.3. Hemocompatibility test

If the percentage of hemolysis is less than 10 %, the materials are called biocompatible. Conversely, if the percentage of hemolysis is below 5%, the materials are called highly hemocompatible. When Fig. 5a and b are examined, it is seen that the hemolysis percentage of nanocomposites synthesized in both THF and acetone media is less than 5%. This means that the nanocomposites are very hemocompatible. Similarly, when comparing the results shown in Fig. 5a and b, it can be said that the materials synthesized in the medium with acetone are more hemocompatible than the materials synthesized in the medium with THF. A similar result was found for chitosan gallate by Cho et al. (2011). They foud that citosan gallate exhibited the protection effect on genomic DNA damage by induced hydroxyl radical, and up-regulated the protein expression of antioxidant enzymes including superoxide dismutase-1 and glutathione reductase under H_2O_2-mediated oxidative stress in RAW264.7 macrophage cells [27].

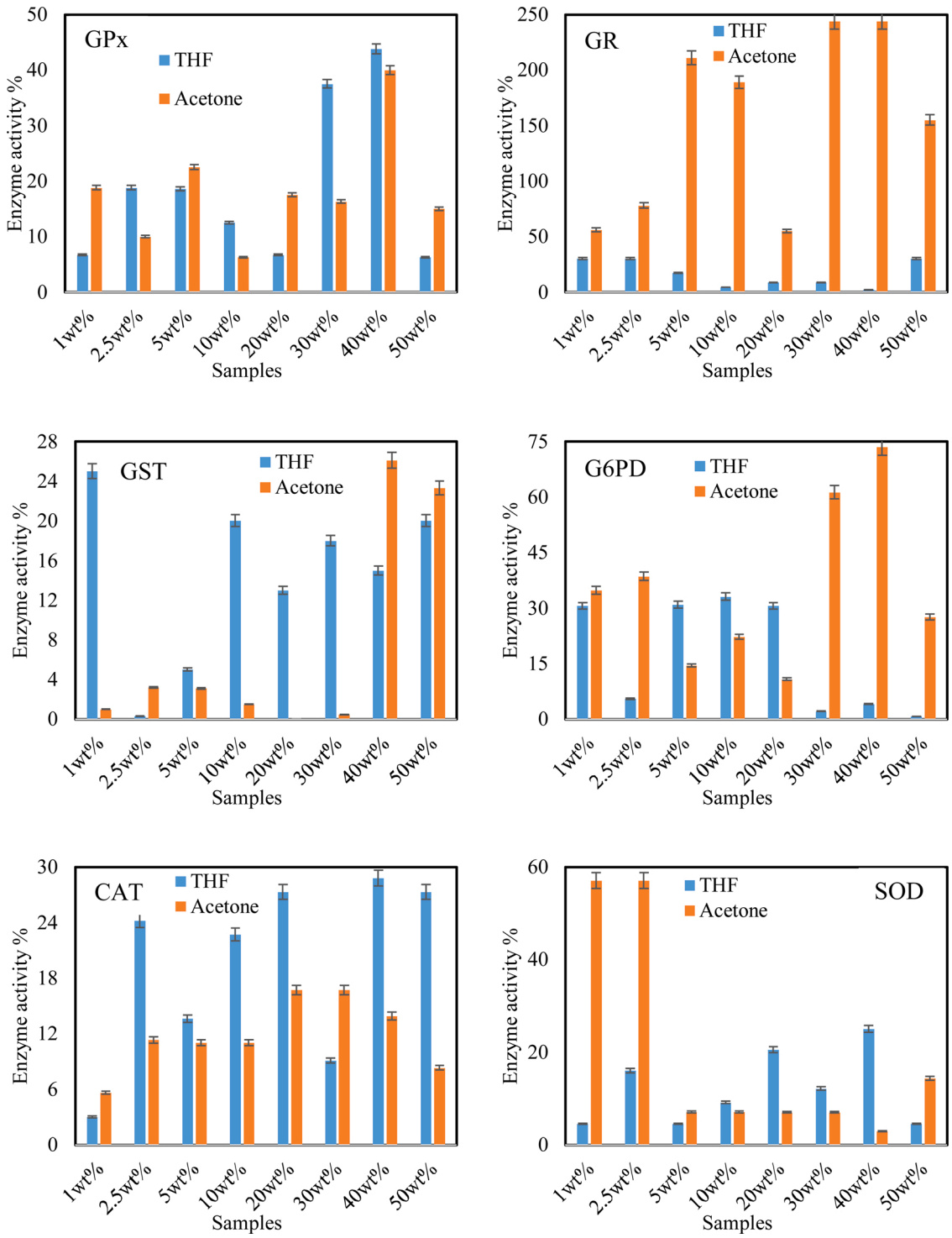

Fig. 4. Percentage effects of biomaterials on antioxidant enzymes.

3.4. Discussion

As can be seen from Fig. 4, the effects of nanocomposites/composites synthesized in different solvent media on antioxidant enzyme activities are different from each other. Nanocomposites/composites synthesized in acetone medium inhibit GPx activity, while those synthesized in THF medium do not have a regular effect on enzyme activity. GPx catalyzes the conversion of reduced glutathione (GSH) to oxidized glutathione (GSSG) in the presence of H_2O_2 as following Eq. (2) [28].

$$2GSH + \underset{\text{Organic hydroperoxide}}{R-O-O-H} \xrightarrow{\text{Glutathione peroxidase}} GSSG + ROH + H_2O \quad (2)$$

GPx is the most abundant in the heart, lung, and brain, and the median level in muscles. In deficiency of this enzyme (for example, for samples synthesized in acetone media), reactive oxygen species (ROSs) increase in the heart, lungs, brain and tissues. These ROSs can undergo structural changes by affecting protein and lipid peroxidation and

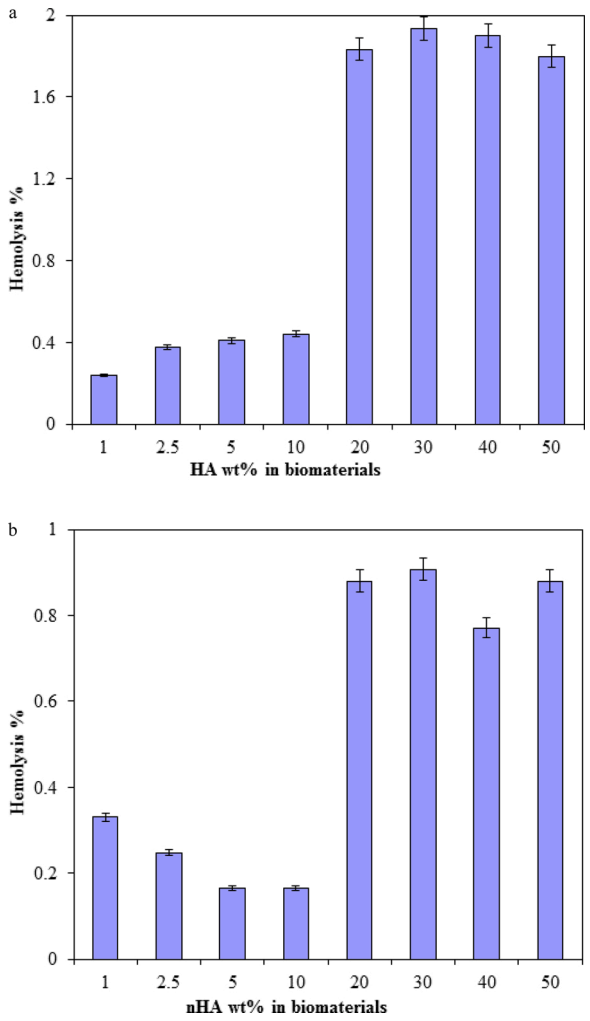

Fig. 5. Hemocompatibility test results of PMMA/HA biomaterials prepared in a) THF and b) acetone solvents.

cellular activities on the plasma membrane. ROSs have the ability to affect membrane activation, protein kinases, growth factors and receptors, signal transduction, oncogen activation and inactivation of repressor genes. This demonstrates that ROS have significant effect on oncogenes and cancer formation. While nanocomposites/composites synthesized in acetone medium have an activator effect on glutathione reductase enzyme, samples synthesized in THF medium do not have a regular effect. GR is a key enzyme of the antioxidative system that protects cells against free radicals. GR catalyzes the conversion of reduced glutathione (GSH) to oxidezed glutathione (GSSG) formed as a result of reduction of hydroperoxides by GPx.

$$GSSG + NADPH + H^{+} \xrightarrow{\text{Glutathione reductase}} 2GSH + NADP^{+} \quad (3)$$

A steady supply of NADPH is therefore vital for erythrocyte integrity [28]. In this study, samples synthesized in acetone medium increase GR activity. If it decreases, decreased GSH/GSSG ratio will contribute to oxidative stress and there is increasing evidence indicating that oxidative stress plays an important role in the pathogenesis of many diseases. The function of GR and balance of the GSH/GSSG ratio are the key factors of various diseases and are awaiting resolution in future researches. During oxidative stress and deficiency of GR, intracellular GSSG accumulates, and the loss of thiol redox balance may cause deleterious consequences for metabolic regulation, cellular integrity, and organ homeostasis. GR inhibition disturbs cellular prooxidant antioxidant balance and may contribute to the genesis of many diseases. The nanocomposites/composites synthesized in both solvent media showed an activator effect on the glutathione-s transferase enzyme. The activity of GSTs is dependent upon a steady supply of GSH from the synthetic enzymes gamma-glutamylcysteine synthetase and glutathione synthetase [29–31]. Increased activity of this enzyme is important in destroying or modifying endogenous toxins formed in cells [32]. Recent studies have reported that the Pi1 isoenzyme of GST has an important role in lung tumorigenesis and is the most abundant GST isoenzyme in the human lung [33]. G6PD, catalyzes net transfer of a hydride ion to $NADP^{+}$ from C1 of glucose-6-phosphate (G6P) to form 6-phosphoglucono-δ-lactone as following Eq. (4):

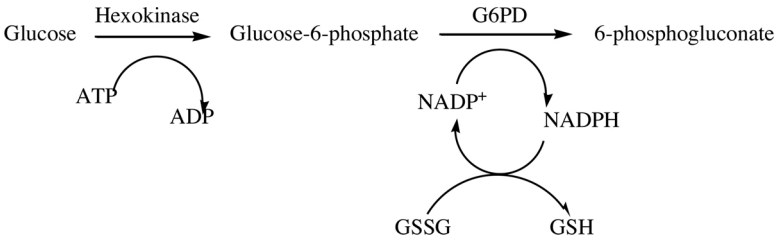

(4)

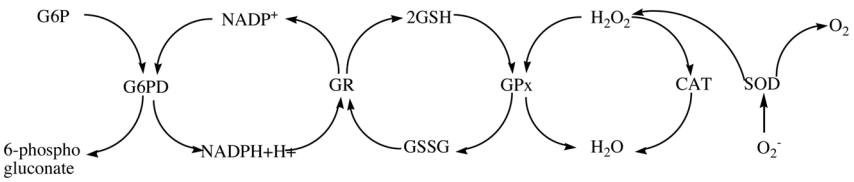

(7)

The effects of nanocomposites and/or composites synthesized in different solvent media on G6PD enzyme activity are different from each other. Samples synthesized in acetone medium showed activator effect while samples synthesized in THF medium showed inhibitory effect. The inhibition of this reaction, catalyzed by G6PD, affects the formation of NADPH and ribose 5-phosphate. NADPH is required for several reductive processes in addition to biosynthesis [28]. SOD is an enzyme that catalyzes the conversion of superoxide free radicals to hydrogen peroxide and molecular oxygen.

$$2O_2^{\bullet} + 2H^{+} \longrightarrow \text{dismutaseSuperoxide} H_2O_2 + O_2 \quad (5)$$

Samples synthesized in acetone medium inhibit SOD activity, while samples synthesized in THF medium do not have a regular effect on SOD activity. A decrease in SOD level increases the formation of free radicals in the cell and causes the development of diseases that cause oxidative damage. CAT is the enzyme that catalyzes the conversion of H_2O_2 to water and molecular oxygen according to the following reaction (6).

$$2H_2O_2 \xrightarrow{\text{Catalase}} 2H_2O + O_2 \quad (6)$$

It has the most activity in the liver and erythrocytes [28]. Samples synthesized in both acetone and THF media inhibit catalase enzyme activity. In general, CAT deficiency increases the likelihood of developing type 2 diabetes.

According to the above explanations, the relationship between antioxidant enzyme activities examined in this study can be demonstrated by the following reaction.

Inadequate of these enzymes implies incomplete production of NADPH in the cell. This case means that sufficient NADPH is not present in the cells to enable the efficient working of antioxidant enzymes involved in the reduction of free radicals [34]. Free radicals can specifically interact with cell membranes and DNA. They lead to rapid damage to the cell by the initiated chain reaction [35]. The main enzyme that eliminates these radicals and allows H_2O_2 formation is SOD enzyme. The forming H_2O_2 is converted to water by the CAT and GPx enzymes, making it completely harmless. GPx requires reduced glutathione (GSH) when it catalyses this reaction and GSH converts to oxidized glutathione (GSSG) at the end of the reaction. GSSG is not involved in detoxification reactions. For this reason, it has to be converted back to GSH. This process is carried out by the GR enzyme, which is dependent on NADPH. NADPH forms as a result of reduction of NADP + by the G6PD enzyme [36]. If G6PD is blocked, it will not be possible to remove harmful free radicals, since NADPH will not be able to be produced, and hemolysis will occur resulting in damage of cell membranes by radicals [37]. Experimental results indicate that some samples have an inhibitory effect on antioxidant enzyme systems. The enzyme activities of living things in contact with these samples diminish, the amount of ROSs increases, and the enzymes can not regularly work. Morever, these PGRs cause to hemolysis of blood in high ratio. As a result, some samples show toxic effects and negatively affect cell metabolism.

3.5. Conclusions

Biomaterials synthesized based on solvent removal method using PMMA and hydroxyapatites were characterized by XRD, FTIR-ATR and DTA/TG. *in vitro* their biocompatibilities and effects on some antioxidant enzymes were investigated. HA was homogeneously distributed in PMMA/HA biomaterials containing HA less than 10 wt%. FTIR-ATR analysis indicated that the interactions between —OH groups in hydroxyapatite and carbonyl groups in PMMA occurred. The increase in thermal stability was compatible with data obtained from FTIR-ATR analysis. Biomaterials prepared in THF medium were more thermally stable than prepared in acetone medium. Nanocomposites and composites had different effects on enzyme activities. Samples synthesized in acetone medium increased enzyme activities as activator for GR and G6PD enzymes, while inhibiting GPx and CAT enzyme activities. On the other hand, samples synthesized in THF medium showed inhibitory behavior for G6PD and CAT enzymes. The effects of samples synthesized in other different media on enzyme activities had not shown regularity. Materials synthesized in the medium with acetone were more hemocompatible than the materials synthesized in the medium with THF. Synthesized materials do not have a significant negative effect on antioxidant enzymes.

CRediT authorship contribution statement

Serap Doğan: Conceptualization, Methodology, Writing - original draft, Writing - review & editing. **Taner Özcan:** Formal analysis, Investigation. **Mehmet Doğan:** Writing - original draft, Writing - review & editing. **Yasemin Turhan:** Investigation.

Declaration of Competing Interest

The authors declare that they have no conflict of interest.

Appendix A. Supplementary data

Supplementary material related to this article can be found, in the online version, at doi:https://doi.org/10.1016/j.enzmictec.2020.109676.

References

[1] M.E. Diken, S. Doğan, Y. Turhan, M. Doğan, Biological properties of PMMA/nHAp and PMMA/3-APT-nHAp nanocomposites, Int. J. Polym. Mater. Polym. Biomater. 67 (13) (2018) 783–791.
[2] B. Yilmaz, S. Doğan, S.E. Kasımoğulları, Hemocompatibility, cytotoxicity, and genotoxicity of poly(methylmethacrylate)/nanohydroxyapatite nanocomposites synthesized by melt blending method, Int. J. Polym. Mater. Polym. Biomater. 67 (6) (2018) 351–360.
[3] Q. Chen, S. Liang, G.A. Thouas, Elastomeric biomaterials for tissue engineering, Prog. Polym. Sci. 38 (3-4) (2013) 584–671.
[4] T. Zhang, W. Cai, F.K. Chu, F. Zhou, S.E. Liang, C. Ma, Y. Hu, Hydroxyapatite/polyurea nanocomposite: preparation and multiple performance enhancements, Compos. Part A. 128 (2020), 105681.
[5] D. Zhou, Q. Dong, K. Liang, W. Xu, Y. Zhou, P. Xiao, Photocrosslinked methacrylated poly(vinyl alcohol)/hydroxyapatite nanocomposite hydrogels with enhanced mechanical strength and cell adhesion, J. Polym. Sci. Part A: Polym. Chem. 57 (2019) 1882–1889.
[6] S. Banerjee, B. Bagchi, S. Bhandary, A. Kool, N.A. Hoque, P. Biswas, K. Pal, P. Thakur, K. Das, P. Karmakar, S. Das, Antimicrobial and biocompatible fluorescent hydroxyapatite-chitosan nanocomposite films for biomedical applications, Colloids Surf. B Biointerfaces 171 (2018) 300–307.
[7] H. Shirali, M. Rafizadeh, A.F. Taromi, E. Jabbari, Fabrication of in situ polymerized poly(butylene succinate-co-ethylene terephthalate)/hydroxyapatite nanocomposite to fibrous scaffolds for enhancement of osteogenesis, J. Biomed. Mater. Res. Part A 105A (2017) 2622–2631.
[8] W.P.S.L. Wijesinghe, M.M.M.G.P.G. Mantilaka, T.S.E.F. Karunarathne, R.M. G. Rajapakse, Synthesis of a hydroxyapatite/poly(methylmethacrylate) nanocomposite using dolomite, Nanoscale Adv. 1 (2019) 86–88.
[9] T.G. Tihan, M.D. Ionita, R.G. Popescu, D. Iordachescu, Effect of hydrophilic-hydrophobic balance on biocompatibility of poly(methyl methacrylate) (PMMA)-hydroxyapatite (HA) composites, Mater. Chem. Phys. 118 (2-3) (2009) 265–269.
[10] J. Zhang, J. Liao, A. Mo, Y. Li, J. Li, X. Wang, Characterization and human gingival fibroblasts biocompatibility of hydroxyapatite/PMMA nanocomposites for provisional dental implant restoration, Appl. Surf. Sci. 255 (2008) 328–330.
[11] S. Doğan, The in vitro effects of some pesticides on carbonic anhydrase activity of Oncorhyncus mykiss and Cyprinus carpio carpio fish, J. Hazard. Mater. A132 (2006) 171–176.
[12] Y. Turhan, Z.G. Alp, M. Alkan, M. Doğan, Preparation and characterization of poly (vinylalcohol)/modified bentonite nanocomposites, Microporous Mesoporous Mater. 174 (2013) 144–153.
[13] E. Beutler, Red Cell Metabolism, 3nd ed, Grune & Stratton, Inc. Orlando, USA, 1984.
[14] W. Habig, M.J. Pabst, W.B. Jakoby, Glutathione S-transferases. The first enzymatic step in mercapturic acid formation, J. Biol. Chem. 249 (22) (1974) 7130–7139.
[15] B.A. Karabulut, E. Özerol, İ. Temel, E.M. Gözükara, Ö. Akyol, Effect of age and smoking on erythrocyte catalase activity and some hematological parameters, J. İnönü Univ. Faculty Med. 9 (2002) 85.

[16] M. Habdous, B. Herbeth, M. Vincent-Viry, J.V. Lamont, P.S. Fitzgerald, S. Visvikis, G. Siest, Serum total antioxidant status, erythrocyte superoxide dismutase and whole-blood glutathione peroxidase activities in the stanislas cohort: influencing factors and reference, Clin. Chem. Lab. Med. 41 (2003) 209.
[17] S. Pan, F. Rasul, W. Li, H. Tian, Z. Mo, M. Duan, X. Tang, Roles of plant growth regulators on yield, grain qualities and antioxidant enzyme activities in super hybrid rice (Oryza sativa L.), Rice 6 (2013) 9.
[18] M.C. Be, Y. Marois, Hemocompatibility, biocompatibility, inflammatoryand in vivo studies of primary reference materials low-density polyethylene and polydimethylsiloxane: a review, J. Biomed. Mater. Res. 58 (5) (2001) 467–477, 2001.
[19] R. Baskaran, S. Selvasekarapadian, N. Kuwata, J. Kawamura, T. Hattori, Conductivity and thermal studies of the blend polymer electrolytes based on PVAC-PMMA, Solid State Ion. 177 (26-32) (2006) 2679–2682.
[20] R. Chandrasekaran, S. Selladurai, J. Solid State Electrochem. 15 (2001) 356.
[21] G. Balasundaram, T.J. Webster, A perspective on nanophase materials for orthopedic implant applications, J. Mater. Chem. 16 (2006) 3737–3745.
[22] R. Benlikaya, Preparation and Characterization of Some Polymethacrylate derivatives/clay Nanocomposites, PhD Thesis, Balikesir University, 2009.
[23] Y. Xu, W.J. Brittain, C. Xue, R.K. Eby, Effect of clay type on morphology and thermal stability of PMMA–clay nanocomposites prepared by heterocoagulation method, Polymer 45 (2004) 3735–3746.
[24] N. Garcia, T. Corrales, J. Guzman, P. Tiemblo, Understanding the role of nanosilica particle surfaces in the thermal degradation of nanosilicaepoly(methyl methacrylate) solution-blended nanocomposites: from low to high silica concentration, Polym. Degrad. Stab. 92 (2007) 635–643.
[25] L.Y. Lie, C.Y. Hsu, K.Y. Hsu, Poly(methylmethacrylate)-silica nanocomposites films from surface-functionalized silica nanoparticles, Polymer 46 (2005) 1851–1856.
[26] C.X. Zhao, W.D. Zhang, Preparation of waterborne polyurethane nanocomposites: polymerization from functionalized hydroxyapatite, Eur. Polym. J. 44 (2008) 1988–1995.
[27] Y.S. Cho, S.K. Kim, J.Y. Je, Chitosan gallate as potential antioxidant biomaterial, Bioorg. Med. Chem. Lett. 21 (10) (2011) 3070–3073.
[28] D. Voet, J.G. Voet, Biochemistry, John Wiley & Sons Inc, US, 2003.
[29] P.D. Josephy, Genetic variations in human glutathione transferase enzymes: significance for pharmacology and toxicology, Hum. Genom. Proteom. (2010), 876940.
[30] J.D. Hayes, J.U. Flanagan, I.R. Jowsey, Glutathione transferases, Annu. Rev. Pharmacol. Toxicol. 45 (2005) 51–88.
[31] M.E. Diken, S. Doğan, M. Doğan, Y. Turhan, In vitro effects of some pesticides on glutathione-s transferase activity, Fresenius Environ. Bull. 26 (12A) (2017) 408–414.
[32] U.H. Danielson, B. Mannervik, Kinetic independence of the subunits of cytosolic glutatione transferase from the rat, Biochem. J. 231 (1985) 263–267.
[33] A.A. Fryer, R. Hume, R.C. Strange, The development of glutathione S-transferase and glutathione peroxidase activities in human lung, Biochim. Biophys. Acta 883 (1986) 448–453.
[34] I. Fridovich, The biology of oxygen radicals, Science 201 (1978) 875.
[35] K. Husain, S.M. Somani, Interaction of exercise and ethanol on hepatic and plasma antioxidant system in rat, Pathophysiology 4 (1997) 69.
[36] S.M. Somani, Exercise, drugs and tissue specific antioxidant system, in: S. M. Somani (Ed.), Pharmacology in Exercise and Sports, CRC Press, Boca Raton, FL, 1996, p. 57.
[37] İ. Ozmen, The effect of some cytotoxic chemicals on glucose 6-phosphate dehydrogenase, SDU J. Sci. (e-journal) 4 (2009) 112.